Soft Matter

COMMUNICATION

View Article Online
View Journal | View Issue

Cite this: *Soft Matter*, 2022, **18**, 5934

Received 28th April 2022,
Accepted 10th July 2022

DOI: 10.1039/d2sm00542e

rsc.li/soft-matter-journal

Thermoresponsive ionogels with switchable adhesion in air and aqueous environments induced by LCST phase behavior†

Cong Zhao,[a] Lie Chen,*[a] Yunfei Ru,[a] Longhao Zhang[a] and Mingjie Liu *[ab]

The rapid development of wearable devices is in urgent demand for materials with switchable adhesion both in air and aqueous environments. Herein, we report a thermoresponsive ionogel with switchable adhesion against various substrates both in air and aqueous environments. The switchable adhesion of ionogels is realized by a phase separation induced collapse of the polymer network and the subsequent extrusion of ionic liquids (ILs) on ionogel surfaces. The hydrophobic poly(butyl acrylate) (PBA) network and ILs endow the ionogels with excellent water-resistance ability, which enables the application of ionogels in aqueous environments. As a result, the adhesion strength of ionogels against rubber can reach an on/off ratio of 75-fold (45 kPa *versus* 0.6 kPa) and 7.7-fold (21 kPa *versus* 2.7 kPa) in air and aqueous environments, respectively. By varying the ratio of two structurally similar ILs in their blends, the responsive temperature of ionogels can be tuned within a wide temperature range from 32 °C to 100 °C. Furthermore, we show a demonstration of an underwater on demand capture and release by taking advantage of the switchable adhesion of ionogels. These nonvolatile ionogels with tunable responsive temperatures and high on/off adhesion strength ratio both in air and aqueous environments show broad applications in the fields related to wearable devices, soft robots and submersible sensors.

Materials possessing switchable adhesion properties in an on-demand manner are of critical interest in practical applications, such as intelligent gripping,[1] flexible electronic devices,[2] human–machine interactions[3–5] and transfer printing.[6] To date, strategies using bioinspired micro- or nano-structure arrays,[7–9] stimuli-responsive polymers[6,10–16] (light-responsive, thermo-responsive, *etc.*) and a combination thereof[17–19] are extensively studied strategies to prepare materials with switchable adhesion. However, for a variety of applications, such as underwater soft robots,[20] submersible soft sensors,[21] and underwater transportation,[1] it is urgent to develop materials with switchable adhesion in aqueous environments. Strategies to realize switchable adhesion in an aqueous environment include host–guest interactions,[22,23] electrostatic interactions,[24] hydrophobic interactions[25] and hierarchical structures that allow suction or capillarity.[18,19,26,27] However, these methods rely on either a pre-modification process or a complex structure design, and thus lack general applicability. Therefore, it is still challenging to develop generally applicable materials with switchable adhesion both in air and aqueous environments.

Here we report a thermoresponsive ionogel with switchable adhesion both in air and aqueous environments. The switchable adhesion of ionogels is induced by a lower critical solution temperature (LCST) phase separation behavior. In the homogeneous state, the hydrophobic dangling chains (butyl side chains) on ionogel surfaces provide high adhesion properties for ionogels. In the phase-separated state, the ionogel exhibits low adhesion due to the collapse of the polymer network and the subsequent extrusion of ionic liquids (ILs) on ionogel surfaces. The ionogel shows excellent switchable adhesion against various substrates such as glasses, poly(tetrafluoroethylene)s (PTFEs), poly(urethane)s (PUs), rubbers and steel. The adhesion strength of ionogels against rubbers can be switched from 45 kPa to 0.6 kPa with 75-fold on/off adhesion strength ratio before and after phase separation. Besides, the switchable adhesion of ionogels is also applicable in an aqueous environment. The hydrophobic PBA network and ILs endow ionogels with excellent water-resistance ability, which can eliminate the interference of water molecules and break the hydrated film on the substrate surfaces. Taking advantage of this feature, we demonstrate respectively the utility of the ionogels with different phase separation temperatures (T_c) for capturing and releasing heavy objects (100 g) in an aqueous environment at different temperatures. Moreover, the good stability of PBA and ILs enables the application of ionogels in harsh aqueous environments, such as HCl (1 M) and NaCl (1 M) solutions. These thermoresponsive ionogels with high on/off

[a] *Key Laboratory of Bio-Inspired Smart Interfacial Science and Technology of Ministry of Education, School of Chemistry, Beihang University, Beijing, 100191, China. E-mail: liumj@buaa.edu.cn, chenlie@buaa.edu.cn*

[b] *International Research Institute for Multidisciplinary Science, Beihang University, Beijing, 100191, China*

† Electronic supplementary information (ESI) available: Details of the method and analysis. See DOI: https://doi.org/10.1039/d2sm00542e

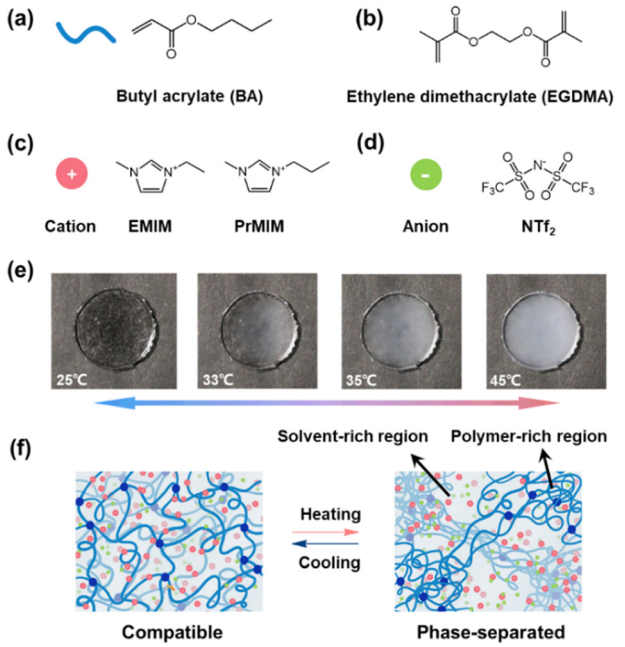

Fig. 1 Design and fabrication of the thermoresponsive ionogels. Molecular structures of the monomer (a), crosslinker (b) and ILs (c and d) used in this work. (e) A series of snapshots for the LCST-type phase behavior of ionogels. (f) Schematic illustration of the mechanism of LCST phase behavior of ionogels.

adhesion strength ratio and excellent switching ability both in air and aqueous environments show broad applications in the field related to wearable devices, soft robots and submersible sensors.

As an extension of the previous work,[28,29] we choose butyl acrylate (BA), a widely used monomer to prepare commercialized adhesives, to construct the polymer network of ionogels. The ionogel is prepared through a one-step polymerization of the BA monomer in imidazolium ILs (1-ethyl-3-methylimidazolium bis(trifluoromethylsulfonyl)imide, [EMIM][NTf_2] and 1-propyl-3-methylimidazolium bis(trifluoromethylsulfonyl)imide, [PrMIM][NTf_2]) using ethyleneglycol dimethacrylate (EGDMA) and diethoxyacetophenone as a crosslinker and a photo-initiator, respectively. Fig. 1a–d show the molecular structures of the monomer, ILs and crosslinker used to prepare ionogels. As a result, the as-prepared ionogel exhibits typical LCST-type phase separation behavior. As shown in Fig. 1e, the transparent PBA/[EMIM][NTf_2] ionogel disc with $T_c \sim 32$ °C quickly becomes opaque with the temperature increased from 25 °C to 45 °C. This thermoresponsive phase behavior of the ionogel is completely reversible. Moreover, the T_c of ionogels can be tuned to exhibit a linear variation within a wide temperature range from 32 °C to 100 °C by varying the ratio of two structurally similar ILs ([PrMIM][NTf_2] and [EMIM][NTf_2]) in their blends (Fig. S1 ESI†). We speculate that the oriented solvation between the polymer and ILs caused by hydrogen-bonding effects and van der Waals interactions may serve as the driving force for the LCST phase behavior in our system. At a temperature below T_c, the ILs selectively solvate the solvatophilic acrylate groups close to the polymer backbone, resulting in a homogeneous and transparent ionogel (Fig. 1f left). As the temperature increases, the hydrogen-bonds and van der Waals interactions between polymer networks and ILs are gradually weakened. When the electrostatic interactions between ILs are stronger than the hydrogen-bonds and van der Waals interactions between polymer networks and ILs, macroscopic phase separation occurs in the ionogels as illustrated in Fig. 1f (right).

It is worth noting that during the microphase separation, the polymer network of ionogels collapses and the ILs will be extruded on ionogel surfaces. This extrusion process of microdroplets is confirmed by microscopic observation. Fig. 2b shows a series of microscope photographs of ionogels during the phase separation. With the heating temperatures above the T_c of ionogels from 25 °C to 35 °C, IL micro droplets are gradually excluded, and aggregate together to form larger droplets on the ionogel surfaces. Moreover, the extruded droplets can be reabsorbed by ionogels during the cooling process. The same phenomenon is observed on the surfaces of samples with T_c of 52 °C and 76 °C, respectively (Fig. S2, ESI†). These results indicate that the extrusion of ILs caused by microphase separation of ionogels is completely reversible.

It is the phase behavior described above that endows ionogels with switchable adhesion. In the homogeneous state, the hydrophobic dangling chains (butyl side chains) on ionogel

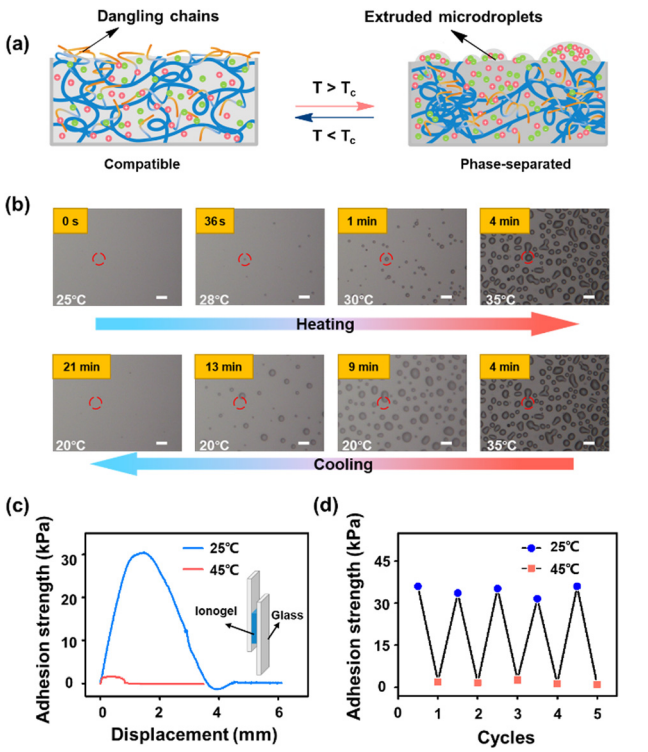

Fig. 2 Phase separation induced switching of adhesion strength of ionogels. (a) Schematic illustration shows the phase separation induced extrusion of micro droplets on ionogel surfaces. (b) Optical microscope images demonstrate the extrusion and reabsorption of micro droplets on the ionogel surface induced by phase separation ($T_c \sim 32$ °C). Scale bar, 20 μm. (c) Adhesion strength – displacement curves of the ionogels at 25 °C and 45 °C respectively measured *via* a lap shear test. Inset: Experimental setup. (d) Cyclic adhesion tests of the ionogels between 25 °C and 45 °C against glass substrates ($T_c \sim 32$ °C).

surfaces provide high adhesion properties for ionogels. The interfacial adhesion is weakened due to the retraction of the butyl side chains on ionogel surfaces when phase separation occurs. Meanwhile, the excluded ILs on ionogel surfaces also act as a lubricant,[30] which decreases the coefficients of friction of ionogels (Fig. S3 ESI†). The switching of adhesion strength of ionogels before and after phase separation is demonstrated through the lap-shear test against glass substrates. As shown in Fig. 2c, the ionogel exhibits a high adhesion strength of up to 30.5 kPa at room temperature (25 °C). Heating to 45 °C (above T_c), the adhesion strength reduces to 1.5 kPa, which is about 20-fold decreased compared with that in the homogenous state. Moreover, cyclic tests are carried out to verify the switching ability of adhesiveness of ionogels. As shown in Fig. 2d, the ionogel retains its strong adhesion after 5 cycles of measurement against glass substrates. These results imply that the ionogel has potential for use in some practical applications that require adhered surfaces that are easily separable for recycling or repair.

We investigate the optimal conditions to prepare ionogels with high adhesion strength by regulating the crosslinking density and polymer content. As shown in Fig. 3a, the adhesion strength of ionogels against glass substrates reaches a maximum (~32 kPa) at a crosslinking density of 0.5 mol%. This trend might be ascribed to the balance between the internal cohesion (strength of ionogels) and the interfacial adhesion because internal cohesion and interfacial adhesion are the main factors that determine the bonding strength between soft matter and substrates. Increasing the crosslinking density (from 0.1 mol% to 0.5 mol%) can promote the internal cohesive forces of the ionogels (Fig. S4, ESI†), resulting in the increase of adhesion strength. However, excessive crosslinking density (>0.5 mol%) in turn will weaken the deformation ability of the polymer network, leading to a significant decrease in the interfacial adhesion strength.[31] Besides, increasing the polymer content will lead to the enhancement of adhesion strength of ionogels. As shown in Fig. 3b, increasing the PBA content from 40 wt% to 90 wt% in PBA/[PrMIM][NTf_2] ionogels, the adhesion strength of ionogels at room temperature increases from 17.7 to 50.1 kPa. This is because on the one hand, the increase of polymer content can enhance the internal cohesion of ionogels. On the other hand, high polymer content can improve interfacial adhesion as well by providing more butyl side chains on the ionogel surfaces. Meanwhile, the polymer content increases the T_cs of ionogels. With the PBA content increasing from 30 wt% to 50 wt%, the T_c of the corresponding ionogel increases from 47 °C to 81 °C (Fig. S5 ESI†). Moreover, the ionogels exhibit high thermal stability, according to our previous work.[28] This feature enables the application of these ionogels in the conditions where a high responsive temperature is required.

To show the universality of current ionogels, the adhesion performance of ionogels against various substrates are investigated by the lap-shear test and the pull-off test. Experimental setups for the lap-shear test and the pull-off test are shown in Fig. 3c and e, respectively. We choose glasses, PTFEs, PUs, rubbers and steel as representative substrates. The adhesion strengths of ionogels against these substrates at 25 °C and 45 °C measured by the lap-shear test are given in Fig. 3d. At 25 °C, the homogeneous ionogels possess a high adhesion strength (>27 kPa) against the substrates. However, the adhesion strength falls sharply when the system is heated above the T_c of ionogels. For PU and rubber substrates, an on/off adhesion strength ratio of 10-fold (165 kPa *versus* 16 kPa for PU, 137 kPa *versus* 13 kPa for rubber) is achieved between two states. It is also found that the adhesion strength of ionogels against glasses is much lower than those of other substrates such as PUs and rubbers. This is because hydrophobicity of the substrate can effectively improve the strength of interfacial adhesion (Fig. S6a, ESI†). PU and rubber substrates have a higher hydrophobicity and roughness (*i.e.* specific surface area), which allow a better interfacial interaction between ionogels and the substrates. Besides, the results of the pull-off test draw a similar conclusion at the applied preload of 33 kPa. As shown in Fig. 3f, the adhesion strength of ionogels against the substrates changed dramatically before and after phase separation. For rubber substrates, a maximum on/off adhesion strength ratio of 75-fold (45 kPa *versus* 0.6 kPa) is achieved between two states. It is worth noting that a 33 kPa preloading in the pull-off test is the optimal condition that enables fully contact between ionogels and the substrates (Fig. S7, ESI†).

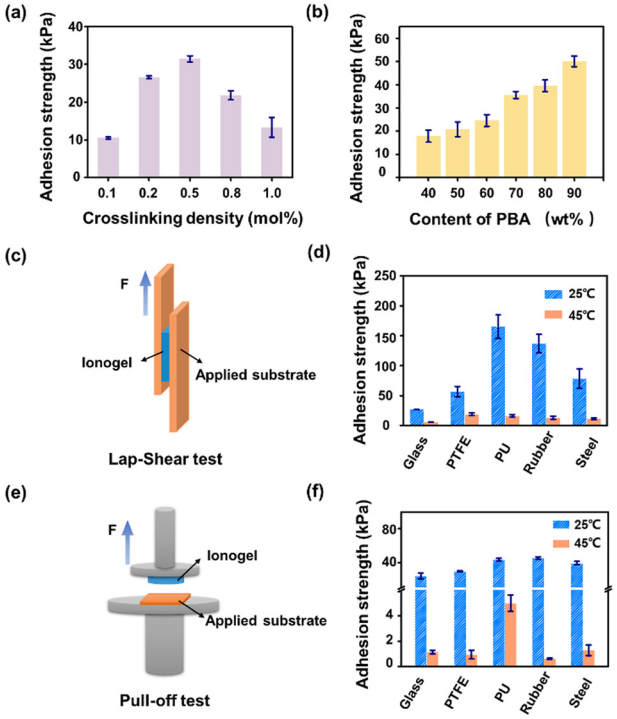

Fig. 3 Thermoresponsive switchable adhesion performance of ionogels. (a) Effect of crosslinking density on adhesion strength of ionogels against glass substrates (in the homogeneous state). (b) Adhesion strength of ionogels as a function of PBA content. (c) Experimental setup for the lap-shear test. (d) The adhesion strength of ionogels (T_c ~ 32 °C) against various substrates at different temperatures measured *via* the lap-shear test. (e) Experimental setup for the pull-off test. (f) The adhesion strength of ionogels (T_c ~ 32 °C) against various substrates at different temperatures measured *via* the pull-off test (preload ~ 33 kPa).

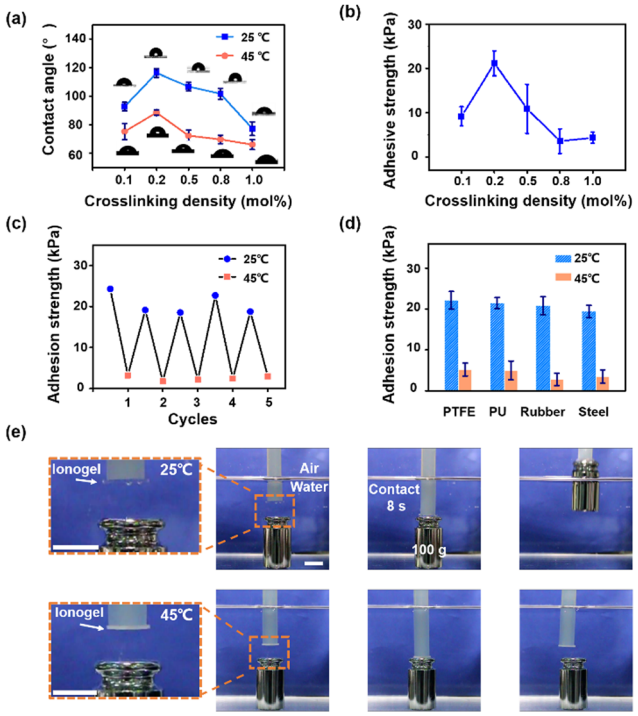

Fig. 4 Underwater switchable adhesion of the ionogels (PBA content: 60 wt%, [EMIM][NTf_2] ILs: 40 wt%). (a) WCAs of ionogels with different crosslinking densities at 25 °C and 45 °C. (b) Underwater adhesion strength of ionogels with different crosslinking densities against glass substrates. (c) Cycling adhesion tests of the ionogels against glass substrates measured *via* the pull-off test. (d) The underwater switchable adhesion of ionogels (T_c ~ 32 °C) against various substrates at different temperatures measured *via* the pull-off test. (e) Photographs show the capture and release behaviors of ionogels in an aqueous environment (T_c ~ 32 °C). Scale bar, 15 mm.

Then, the switchable adhesion of ionogels in an aqueous environment is investigated. We first characterize the water contact angles (WCAs) of ionogels (T_c ~ 32 °C) before and after the phase separation. As shown in Fig. 4a, the homogeneous ionogels (at 25 °C) show stable hydrophobicity (WCAs above 80°) benefiting from the fully hydrophobic compositions (PBA network and hydrophobic ILs) in ionogels. Heating to 45 °C, the WCAs of phase separated ionogels decreased due to the surface energy enhancement of ionogels caused by the extrusion of ILs on ionogel surfaces.[32] In addition, it is found that the WCA reaches a maximum (116°) at a crosslinking density of 0.2 mol% (at 25 °C). This may be ascribed to the balance between the surface rigidity of ionogels and the solvent binding ability of the PBA network. On the one hand, reducing the crosslinking density of polymer network results in a low surface rigidity of ionogels. When a liquid droplet (*e.g.* water) that is immiscible with the substrate is placed on the ionogel surfaces, a higher surface-wetting ridge can be achieved on the ionogel surfaces with lower surface rigidity (*i.e.* better deformability)[33] thus, yielding a higher WCA for an ionogel with lower crosslinking density. On the other hand, an excessively low crosslinking density (0.1 mol%) will weaken the solvent binding ability of PBA network, which will inevitably lead to a leakage of solvent (even if it is a small amount). The leaked solvents on ionogel surfaces will enhance the surface energy of ionogels, leading to a lower WCA on ionogel surfaces. Meanwhile, the underwater adhesion strength of ionogels against glass substrates exhibits the same trend with the WCA as increasing the crosslinking density of ionogels (Fig. 4b). A maximum adhesion strength of 22 kPa is achieved at a crosslinking density of 0.2 mol%. Besides, the adhesion performance of ionogels against glass substrates with different wettability are investigated (Fig. S6b, ESI†). It is found that hydrophobicity of the substrates can effectively improve the strength of underwater interfacial adhesion. These results indicate that the underwater adhesion strength is mainly related to the hydrophobicity of ionogels and substrates. A better hydrophobicity can eliminate the interference of water molecules and break the hydrated film on the substrate surfaces, allowing full contact between the ionogels and the substrates.

These ionogels show excellent switchable adhesion in an aqueous environment. As shown in Fig. 4c, the ionogel retains its strong adhesion after 5 cycles of measurement against glass substrates in an aqueous environment. Besides, the ionogel also exhibits high adhesion strength (~20 kPa) against substrates such as PTFEs, PUs, rubbers and steel in the homogeneous state. Heating above the T_c, the adhesion strength of ionogels against these substrates sharply decreases (Fig. 4d). The on/off ratio of adhesion strength against the rubber substrate is about 7.7-fold (21 kPa *versus* 2.7 kPa). Furthermore, we show the demonstration of an underwater on demand capture and release of the target object by taking advantage of the switchable adhesion of ionogels. As shown in Fig. 4e, an ionogel disc (2 mm in thick, 15 mm in diameter) with T_c ~ 32 °C is utilized to carry out this demonstration. At 25 °C below the T_c, a 100 g object can be lifted using the ionogel disc through an 8 s contact in an aqueous environment. In contrast, the ionogel disc fails to lift the same object at 45 °C above the T_c. Moreover, ionogels with higher T_cs (*e.g.* 52 °C and 76 °C) can also be utilized for the underwater on demand capture and release (Fig. S8 and S9, ESI†). We suppose that the tunable responsive temperature of current ionogels can meet the requirements for diverse practical applications. In practical applications, the underwater adhesion process might be operated under different aqueous conditions. Therefore, we further investigate the adhesion strength of ionogels in acid and salt solutions. It is found that the ionogels can maintain a high adhesion strength against hydrophobic substrates such as PTFEs and PUs (20.6 ± 2.7 kPa, 21.7 ± 3.1 kPa, respectively) in a 1 M NaCl solution, which is comparable to underwater adhesion (Fig. S10a ESI†). In a strong acid (1 M) solution, the adhesion strength of ionogels against PTFEs and PUs is 18.6 ± 5.1 kPa and 18.5 ± 3.1 kPa, respectively (Fig. S10b ESI†). These results indicate that the ionogel can be applied in harsh aqueous environments.

Conclusions

In this work, we report a thermoresponsive ionogel with switchable adhesion against various substrates both in air and aqueous environments. This transition of ionogels is realized by a

phase separation induced collapse of polymer network and the subsequent extrusion of ILs on ionogel surfaces. The hydrophobic polymer network and ILs endow the ionogels with excellent water-resistance, which enables the application of ionogels in aqueous environments. As a result, these ionogels exhibit a high on/off adhesion strength ratio and excellent switching ability both in air and aqueous environments. In addition, by varying the ratio of two structurally similar ILs in their blends, the responsive temperature of ionogels can be tuned within a wide temperature range from 32 °C to 100 °C. Thus, these ionogels can meet the requirements of different response temperatures in practical applications. These nonvolatile ionogels with tunable responsive temperatures and high on/off adhesion strength ratio both in air and aqueous environments could be broadly applied in the fields related to wearable devices, soft robots and submersible sensors.

Conflicts of interest

There are no conflicts of interest to declare.

Acknowledgements

This work was financially supported by the National Natural Science Fund for Distinguished Young Scholars (No. 21725401), the National Key R&D Program of China (Grant 2017YFA0207800), and the National Natural Science Foundation (22161142021).

Notes and references

1 Y. Ma, S. Ma, Y. Wu, X. Pei, S. N. Gorb, Z. Wang, W. Liu and F. Zhou, *Adv. Mater.*, 2018, **30**, 1801595.
2 D.-H. Kim, N. Lu, R. Ma, Y.-S. Kim, R.-H. Kim, S. Wang, J. Wu, S. M. Won, H. Tao, A. Islam, K. J. Yu, T.-I. Kim, R. Chowdhury, M. Ying, L. Xu, M. Li, H.-J. Chung, H. Keum, M. McCormick, P. Liu, Y.-W. Zhang, F. G. Omenetto, Y. Huang, T. Coleman and J. A. Rogers, *Science*, 2011, **333**, 838–843.
3 J. Sun, Y. Yuan, G. Lu, L. Li, X. Zhu and J. Nie, *J. Mater. Chem. C*, 2019, **7**, 11244–11250.
4 H. Ko and A. Javey, *Acc. Chem. Res.*, 2017, **50**, 691–702.
5 Y. X. Liu, L. Chen, Z. G. Zhao, R. C. Fang and M. J. Liu, *Acta Polym. Sin.*, 2018, **0**, 1155–1174.
6 T.-H. Lee, G.-Y. Han, M.-B. Yi, H.-J. Kim, J.-H. Lee and S. Kim, *ACS Appl. Mater. Interfaces*, 2021, **13**, 43364–43373.
7 M. D. Bartlett, A. B. Croll, D. R. King, B. M. Paret, D. J. Irschick and A. J. Crosby, *Adv. Mater.*, 2012, **24**, 1078–1083.
8 L. Xue, A. Kovalev, K. Dening, A. Eichler-Volf, H. Eickmeier, M. Haase, D. Enke, M. Steinhart and S. N. Gorb, *Nano Lett.*, 2013, **13**, 5541–5548.
9 L. Heepe and S. N. Gorb, *Annu. Rev. Mater. Res.*, 2014, **44**, 173–203.
10 T. J. Gately, W. Li, S. H. Mostafavi and C. J. Bardeen, *Macromolecules*, 2021, **54**, 9319–9326.
11 J. Cui, D.-M. Drotlef, I. Larraza, J. P. Fernández-Blázquez, L. F. Boesel, C. Ohm, M. Mezger, R. Zentel and A. del Campo, *Adv. Mater.*, 2012, **24**, 4601–4604.
12 S. Reddy, E. Arzt and A. del Campo, *Adv. Mater.*, 2007, **19**, 3833–3837.
13 M. Frensemeier, J. S. Kaiser, C. P. Frick, A. S. Schneider, E. Arzt, R. S. Fertig III and E. Kroner, *Adv. Funct. Mater.*, 2015, **25**, 3013–3021.
14 H. Ko, Z. Zhang, Y.-L. Chueh, E. Saiz and A. Javey, *Angew. Chem., Int. Ed.*, 2010, **49**, 616–619.
15 L. Chen, Y. A. Yin, Y. X. Liu, L. Lin and M. J. Liu, *Chin. J. Polym. Sci.*, 2017, **35**, 1181–1193.
16 Z. G. Zhao, Y. C. Xu, R. C. Fang and M. J. Liu, *Chin. J. Polym. Sci.*, 2018, **36**, 683–696.
17 D.-M. Drotlef, P. Blümler and A. del Campo, *Adv. Mater.*, 2014, **26**, 775–779.
18 H. Lee, D.-S. Um, Y. Lee, S. Lim, H.-J. Kim and H. Ko, *Adv. Mater.*, 2016, **28**, 7457–7465.
19 H. Lee, B. P. Lee and P. B. Messersmith, *Nature*, 2007, **448**, 338–341.
20 H. Yuk, S. Lin, C. Ma, M. Takaffoli, N. X. Fang and X. Zhao, *Nat. Commun.*, 2017, **8**, 14230.
21 Z. Yu and P. Wu, *Adv. Mater.*, 2021, **33**, 2008479.
22 Y. Ahn, Y. Jang, N. Selvapalam, G. Yun and K. Kim, *Angew. Chem., Int. Ed.*, 2013, **52**, 3140–3144.
23 G. Ju, M. Cheng, F. Guo, Q. Zhang and F. Shi, *Angew. Chem., Int. Ed.*, 2018, **57**, 8963–8967.
24 H. Fan, J. Wang, Z. Tao, J. Huang, P. Rao, T. Kurokawa and J. P. Gong, *Nat. Commun.*, 2019, **10**, 5127.
25 L. Han, M. Wang, L. O. Prieto-López, X. Deng and J. Cui, *Adv. Funct. Mater.*, 2020, **30**, 1907064.
26 P. Glass, H. Y. Chung, N. R. Washburn and M. Sitti, *Langmuir*, 2010, **26**, 17357–17362.
27 L. Xue, A. Kovalev, A. Eichler-Volf, M. Steinhart and S. N. Gorb, *Nat. Commun.*, 2015, **6**, 6621.
28 L. Chen, C. Zhao, X. Duan, J. Zhou and M. Liu, *CCS Chem.*, 2021, **3**, 1659–1669.
29 L. Chen, J. Huang, C. Zhao, J. J. Zhou and M. J. Liu, *Chin. J. Polym. Sci.*, 2020, **39**, 585–591.
30 Y. Zhou and J. Qu, *ACS Appl. Mater. Interfaces*, 2017, **9**, 3209–3222.
31 J. Li, A. D. Celiz, J. Yang, Q. Yang, I. Wamala, W. Whyte, B. R. Seo, N. V. Vasilyev, J. J. Vlassak, Z. Suo and D. J. Mooney, *Science*, 2017, **357**, 378–381.
32 L. P. Wen, Y. Tian and L. Jiang, *Angew. Chem., Int. Ed.*, 2015, **54**, 3387–3399.
33 Z. Hao, A. Ghanekarade, N. Zhu, K. Randazzo, D. Kawaguchi, K. Tanaka, X. Wang, D. S. Simmons, R. D. Priestley and B. Zuo, *Nature*, 2021, **596**, 372–376.

